AMERICAN SOCIETY FOR MICROBIOLOGY | Antimicrobial Agents and Chemotherapy®

MECHANISMS OF RESISTANCE

Proximal Binding Pocket Arg717 Substitutions in *Escherichia coli* AcrB Cause Clinically Relevant Divergencies in Resistance Profiles

Martijn Zwama,[a] Kunihiko Nishino[a,b,c]

[a]SANKEN (The Institute of Scientific and Industrial Research), Osaka University, Ibaraki, Osaka, Japan
[b]Graduate School of Pharmaceutical Sciences, Osaka University, Suita, Osaka, Japan
[c]Center for Infectious Disease Education and Research, Osaka University, Suita, Osaka, Japan

ABSTRACT Recent mutations in RND efflux pumps in clinical strains have further increased multidrug resistance. We show that R717L and R717Q substitutions (found in azithromycin-resistant *Salmonella enterica* spp.) in the *Escherichia coli* efflux pump AcrB dramatically increase macrolide, as well as fluoroquinolone, resistance. On the other hand, cells became more susceptible to novobiocin and β-lactam cloxacillin. We urge the control of, and adjustments to, treatments with antibiotics and the need for novel antibiotics and efflux pump inhibitors.

KEYWORDS antimicrobial resistance, multidrug resistance, RND, AcrB, macrolides, fluoroquinolones

Multidrug-resistant pathogens resist multiple antibiotics (1–4), which can be caused by over-expressed intrinsic and acquired (5–7) efflux pumps (5, 8, 9). In Gram-negative bacteria, RND-type efflux pumps (7, 10) attribute to multidrug resistance (MDR) by expelling structurally unrelated antibiotics (11). Recently, amino acid substitutions further increased resistance (12). Substitutions in the proximal binding pocket (PBP, Fig. 1) (11–14) of *Salmonella enterica* Serovars Typhi and Paratyphi A pump AcrB caused azithromycin (AZM)-resistant phenotypes (12). This is concerning, as AZM is often the last available typhoid treatment option (15, 16). In 2010, AZM-resistant *S.* serovars Paratyphi A strains from Pakistan were first reported (17). The AZM breakpoint has been determined to be $>$16 μg/mL for *S. Typhi*. (18). Hooda et al. (2019) first described R717Q/L substitutions in AcrB from *Salmonella* isolates from Bangladesh. Multiple strains harboring R717Q/L showed AZM resistance between 32–64 μg/mL (19). R717Q/L were also found in AZM-resistant *S. Typhi* strains from Nepal (15), Pakistan (16), and India (20). Phylogenetic analysis showed the R717Q mutation likely spontaneously and independently emerged (16). Sajib et al. (2021) showed that most AZM-resistant Typhi and Paratyphi A strains from Bangladesh had these substitutions. They predicted that the first Arg717 substitutions emerged around 2010 and that a travel-related R717Q mutant was also found in the United Kingdom (21). Additionally, after analysis of a similar R714G substitution in MtrD from *Neisseria gonorrhoeae* (22), different substitutions (R714C/H/L) were found in some AZM-resistant isolates (23). Here, we investigated R717Q/L in *Escherichia coli* AcrB (AcrB-Ec), closely related to *Salmonella* AcrB, expressed in *E. coli*. We compared the effects to other clinical mutations, namely, K823E/N (causing enhanced AZM resistance by MtrD) (22–25) and G288D (causing fluoroquinolone resistance in a *S. Typhimurium* clinical strain) (26).

S. enterica (Typhi and Paratyphi A) AcrB and AcrB-Ec comprise 1,049 amino acids (Fig. S1 in the supplemental material) and share about 94% identity (Fig. S2–S4) (27). R717Q/L side chains are shorter and more hydrophobic than Arg717 (Fig. 1c, S5). Mutant and wild-type AcrB-Ec were equally expressed (Fig. S6). Table 1 shows the agar-plate (solid)

Copyright © 2022 Zwama and Nishino. This is an open-access article distributed under the terms of the Creative Commons Attribution 4.0 International license.

Address correspondence to Martijn Zwama, m.zwama@sanken.osaka-u.ac.jp, or Kunihiko Nishino, nishino@sanken.osaka-u.ac.jp.

The authors declare no conflict of interest.

[This article was published on 21 March 2022 with an incorrect e-mail address for Martijn Zwama in the PDF. The address was corrected in the current version, posted on 28 March 2022.]

Received 20 December 2021
Returned for modification 20 January 2022
Accepted 10 February 2022
Published 21 March 2022

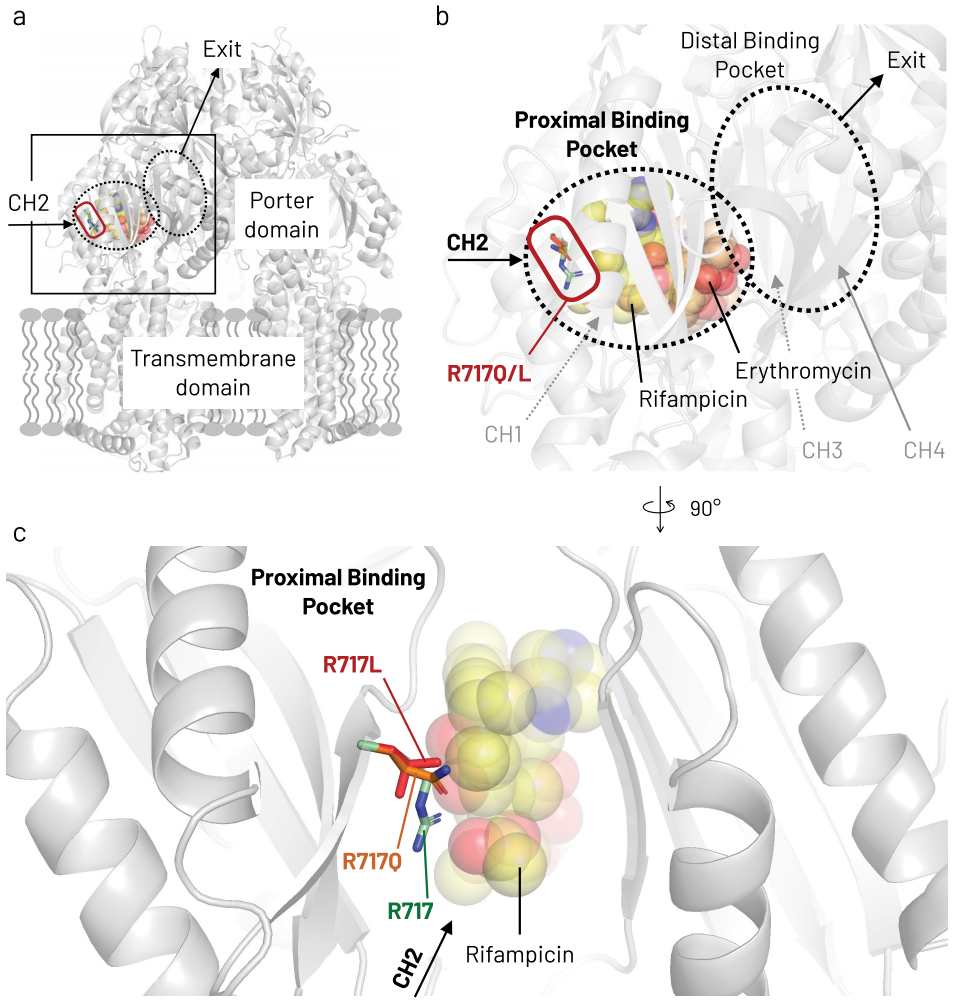

FIG 1 Location of Arg717 and the R717Q/L amino acid substitutions in AcrB-Ec. (a) Side view of the entire AcrB-Ec trimer. (b) A close-up view of the rectangle area highlighted in panel a. Two drug molecules are present in the proximal binding pocket (rifampicin and erythromycin). The Arg717 residue and the R717Q/L substitutions are located at the entrance of the pocket. (c) Close-up inwards view of the proximal binding pocket and Arg717 area. Rifampicin can be seen behind the Arg717 residue and the R717Q/L substitutions. CH1–4, Channel 1–4. Colors: red box, substitution area; yellow spheres, rifampicin; orange spheres, erythromycin; green sticks, Arg717; orange sticks, R717Q; red sticks, R717L. PDB accession codes: 4DX5 (for the main structure and the mutagenesis); 3AOC (for the erythromycin coordinates); 3AOD (for the rifampicin and the wild-type Arg717 side chain coordinates).

MIC results of 20 compounds. Compared to wild-type AcrB, R717Q/L give divergent resistance spectra. MICs generally increased for macrolides and fluoroquinolones but decreased for novobiocin (NOV) and β-lactam cloxacillin (CLX). For clarithromycin (CLR) and erythromycin (ERY), the MICs of R717Q/L were $>$256 and 256 μg/mL, respectively, compared to 128 μg/mL for the wild type. The MIC for AZM increased significantly by 4- and 8-fold for R717Q and R717L (64 and 128 μg/mL, compared to 16 μg/mL for wild-type AcrB). Mutant cells grew as full and healthy colonies on the agar plates at their highest viable macrolide concentrations. Ofloxacin (OFX), levofloxacin (LVX), and moxifloxacin (MXF) MICs increased 2-fold. For R717Q, the monobactam aztreonam (ATM) MIC increased by 4-fold. R717L increased the ethidium bromide (EtBr) MIC 2-fold. Interestingly, R717Q and R717L both caused 2-fold NOV and CLX MIC decreases.

To compare the R717Q/L mutations, we introduced other clinical substitutions in AcrB-Ec, found in *N. gonorrhoeae* MtrD and *S. Typhimurium* AcrB. In MtrD, K823E/N were observed in macrolide-resistant strains (22–25). In AcrB, G288D conferred increased fluoroquinolone resistance in a clinical strain (26). Therefore, we introduced the substitutions G288D, E826K, and E826N in AcrB-Ec. Lys823 in MtrD corresponds to Glu826 in AcrB-Ec

TABLE 1 Antimicrobial susceptibility of AcrB-Ec expressing cells with several amino acid substitutions[a]

	Minimum inhibitory concn (MIC) (μg mL^{-1})[b]																			
	Planar aromatic cations					Macrolides			β-lactams		Quinolones						Other		Bile salts	
Strain[c]	EtBr	MtB	ACR	CV	BZK	ERY	AZM	CLR	CLX	ATM	NAL	NOR	CIP	OFX	LVX	MXF	NOV	MIN	Mix	DEOX
Vector	16	16	16	2	4	2	<0.5	2	1	1/16	1	1/128	1/256	1/64	1/128	1/256	4	0.125	2,500	625
WT	512	>1,024	256	8–16	128	128	16	128	256	1/32	4	1/32	1/64	1/16	1/32	1/16	256	1	>20,000	10,000
R717Q	512	>1,024	256	8	128	**256**	**64**	>**256**	*128*	**0.125**	4	1/32	1/64	**0.125**	**1/16**	**0.125**	*128*	1	>20,000	10,000
R717L	**1,024**	>1,024	256	8	128	**256**	**128**	>**256**	*128*	1/32	4	1/32	1/64	**0.125**	1/32	**0.125**	*128*	1	>20,000	10,000
G288D	*256*	*1,024*	*128*	8	*64*	*64*	*4*	*64*	*128*	**0.125**	4	1/32	1/64	1/16	1/32	1/16	*64*	1	>20,000	**20,000**
E826K	512	>1,024	*128*	8	128	128	*4*	*64*–128	256	**1/16**	4	1/32	1/64	1/16	1/32	1/16	256	1	>20,000	10,000
E826N	512	>1,024	256	8	128	128	16	128	256	**1/16**	4	1/32	1/64	1/16	1/32	1/16	256	1	>20,000	**20,000**

[a]EtBr, ethidium bromide; MtB, methylene blue; ACR, acriflavine; CV, crystal violet; BZK, benzalkonium; ERY, erythromycin; AZM, azithromycin; CLR, clarithromycin; CLX, cloxacillin; ATM, aztreonam; NAL, nalidixic acid; NOR, norfloxacin; CIP, ciprofloxacin; OFX, ofloxacin; LVX, levofloxacin; MXF, moxifloxacin; NOV, novobiocin; MIN, minocycline; Mix, bile sale mixture; DEOX, deoxycholate; WT, wild-type AcrB-Ec.

[b]His-tagged wild-type AcrB-Ec and mutant AcrB-Ec were expressed from pBAD33 plasmids and expressed in MG1655Δ*acrB* cells, MIC values determined by serial dilution agar plates. Bold indicates a 2-fold increase in MIC, bold underlined indicates a 4-fold or more increase in MIC, and italic indicates a decrease of 2-fold or more in MIC compared to wild-type.

[c]Strain information: all strains are *Escherichia coli* MG1655Δ*acrB* with different plasmids, namely Vector, pBAD33; WT, pBAD33acrBhis; rest, pBAD33acrBhis with the respective amino acid substitution.

(Fig. S7); thus, we introduced the K823E "reversed" substitution in AcrB-Ec. This residue lies deeper in the PBP "behind" Arg717 (13, 22). Gly288 is a distal binding pocket residue (Fig. 1b), close to the hydrophobic pit, where multiple drugs bind in the binding monomer (13, 22, 28–33). Results are shown in Table 1. G288D decreased most planar aromatic cation (PAC), macrolide, β-lactam CLX, and NOV MICs. Contrarily, G288D increased ATM and deoxycholate (DEOX) MICs by 4- and 2-fold, respectively. E826K increased susceptibility for acriflavine (ACR) and AZM (and slightly for CLR); however, MICs were 2-fold higher for ATM. E826N MICs for ATM and DEOX increased by 2-fold. The increased susceptibility of AcrB-Ec(E826K) cells to ACR, AZM, and CLR could correspond with the decreased susceptibility to AZM (23) and ERY (22, 24) for strains harboring the mutated MtrD(K823E).

Solid plate MICs (Table 1) showed an up to 8-fold increase in macrolide MICs for R717Q/L mutants. Furthermore, clinically relevant G288D generally caused decreased MICs. The reversed substitution E826K decreased multiple drugs' MICs. Thus, the 8-fold AZM, the 2-fold ERY, and the $\geq$4-fold CLR MIC increases show a significant macrolide export gain-of-function for AcrB-Ec by the R717Q/L substitutions. Therefore, we checked the growth of R717Q/L cells in macrolide, CLX, and NOV supplemented liquid medium. Fig. 2 (macrolides) shows that wild-type cell growth is significantly inhibited at 256 μg/mL and completely inhibited at 512 μg/mL ERY (top lane). Contrarily, R717Q/L mutants grow fully at 256 μg/mL and significantly grow even under 512 μg/mL. Similarly, for CLR (middle lane), wild-type cell growth is inhibited at 256 μg/mL, while mutant cells can grow fully. At 512 μg/mL, mutant cells still slightly grow. For AZM (bottom lane), wild-type cell growth was already partly inhibited at 16 μg/mL and fully at 32 μg/mL. Contrarily, mutants could fully grow, even in 64 μg/mL (even in 128 μg/mL, the mutants seem very slightly viable). These results corroborate the significant resistance increase caused by R717Q/L for macrolides, especially AZM. Under all conditions, R717L seemed somewhat more viable than R717Q. Fig. 3 shows inhibited cell growth for R717Q/L, compared to the wild type, in CLX and NOV supplemented medium, corroborating the plate MIC results (Table 1).

To further check the clinical significance, we performed Kirby-Bauer disk diffusion susceptibility tests. Table 1 shows R717Q/L also increased fluoroquinolone resistance, besides increased macrolide resistance. *S. Typhi* strains from Pakistan and Nepal show that R717Q/L cause reduced fluoroquinolone susceptibility; however, they note a double mutation in *gyrA* contributes to this phenotype (15, 16). Nonetheless, we wanted to further investigate the consequences of R717Q/L in AcrB-Ec on fluoroquinolone and macrolide resistance. Fig. 4 shows the disk diffusion susceptibility results for macrolides, fluoroquinolones, NOV, and minocycline (MIN). When AcrB-Ec is expressed, the inhibition zones for all compounds decrease (Fig. 4, WT versus KO). R717Q/L mutations significantly decrease the inhibition zones further for all macrolides and fluoroquinolones (visible by

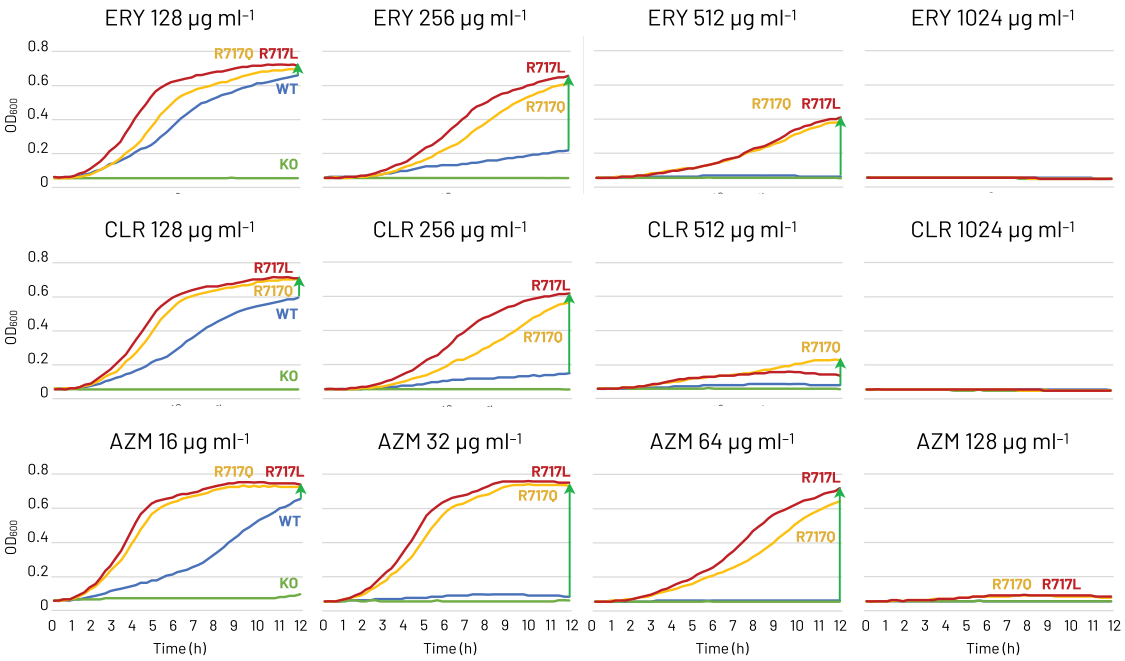

FIG 2 Growth ability of *E. coli* MG1655Δ*acrB* cells expressing wild-type, R717Q, and R717L mutant AcrB-Ec under several macrolide concentrations. Top lane, growth ability under erythromycin; middle lane, under clarithromycin; bottom lane, under azithromycin. Blue, yellow, red, and green indicate wild-type AcrB, R717Q mutant, R717L mutant, and vector only, respectively. The green arrow mark indicates the increase in growth ability of the mutant strains compared to the wild-type strain. ERY, erythromycin; CLR, clarithromycin; AZM, azithromycin. Experiments repeated twice provided similar results; shown is one of the results.

the naked eye in Fig. 4a, quantified in Fig. 4b). R717L has slightly more impact on the inhibition zone decreases than R717Q (Fig. 4b). Interestingly, R717L also decreases the inhibition zone for MIN. Similar to Table 1 and Fig. 3, R717Q/L increased NOV susceptibility (Fig. 4a and b).

We showed that R717Q/L substitutions in AcrB-Ec confer significant increased macrolides resistance, with an up to 8-fold increase in MICs. These findings corroborate the phenotypes of AZM-resistant *S. Typhi* and Paratyphi A strains harboring the R717Q/L mutations (19–21). Interestingly, R717Q/L caused a 2-fold MIC decrease for CLX and NOV. This could (partly) explain the susceptibility of AZM-resistant *S. Typhi* R717Q strains from Pakistan, which were still susceptible to third-generation cephalosporins

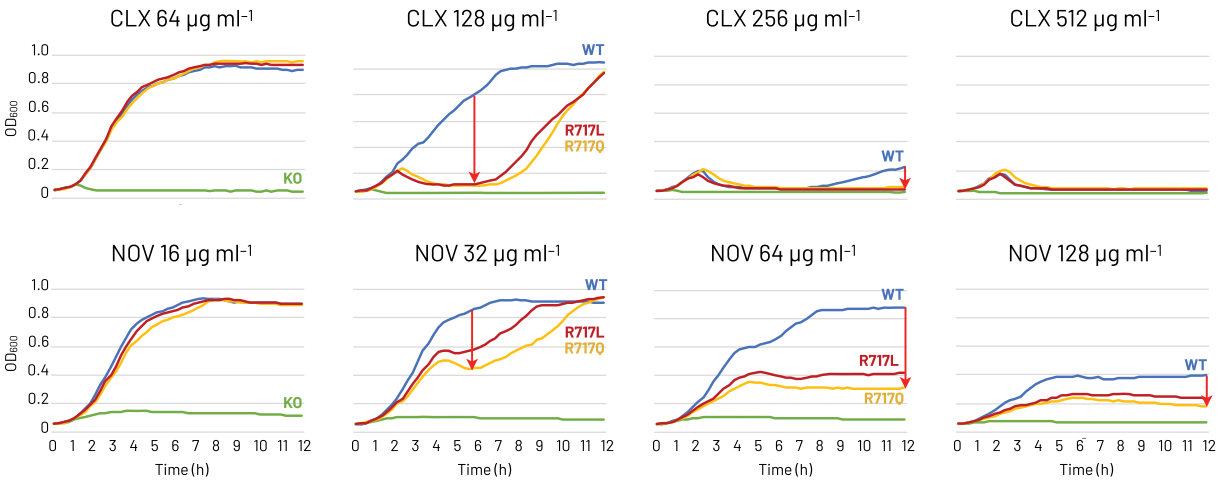

FIG 3 Growth ability of *E. coli* MG1655Δ*acrB* cells expressing wild-type, R717Q, and R717L mutant AcrB-Ec under cloxacillin and novobiocin. Top lane, growth ability under cloxacillin; bottom lane, under novobiocin. Blue, yellow, red, and green indicate wild-type AcrB, R717Q mutant, R717L mutant, and vector only, respectively. The red arrow mark indicates the decrease in growth ability of the mutant strains compared to the wild-type strain. CLX, cloxacillin; NOV, novobiocin. Experiments repeated twice provided similar results; shown is one of the results.

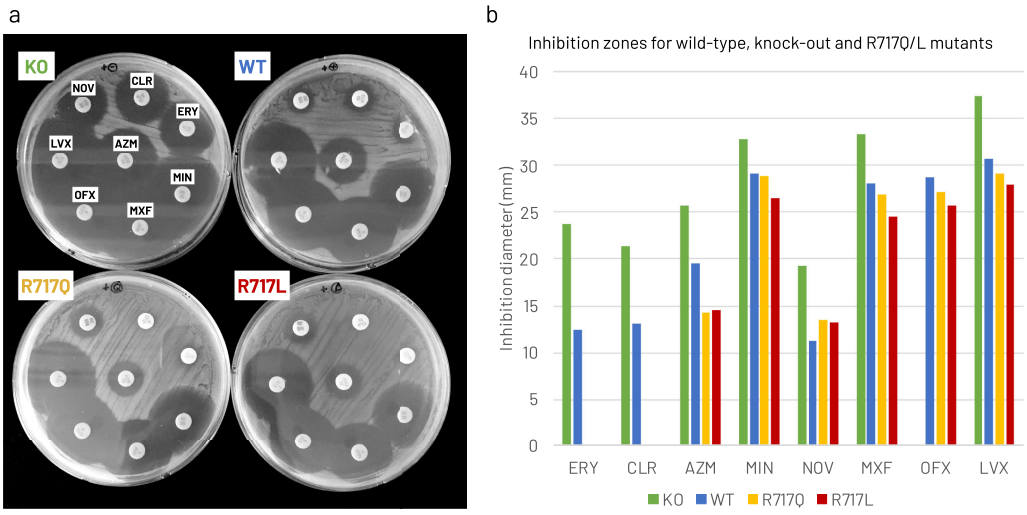

FIG 4 Kirby-Bauer disk diffusion susceptibility testing of *E. coli* MG1655Δ*acrB* cells expressing wild-type, R717Q, and R717L mutant AcrB-Ec under various antibiotics. (a) Grayscale images of knockout, wild-type, and mutant *E. coli* grown on Mueller-Hilton agar plates, supplemented with resazurin and arabinose. Disks with specific antibiotics of interest can be seen on all four plates, along with the growth inhibition zones around the disks. (b) Quantification of the inhibition zones. The vertical axis shows the inhibition diameter in mm. Growth of the cells up to the antibiotic disk is denoted as 0 mm. (a–b) Blue, yellow, red, and green indicate wild-type AcrB, R717Q mutant, R717L mutant, and vector only, respectively. KO, *acrB* knockout (vector only); WT, wild-type; ERY, erythromycin; CLR, clarithromycin; AZM, azithromycin; NOV, novobiocin; LVX, levofloxacin; OFX, ofloxacin; MXF, moxifloxacin; MIN, minocycline. Shown is one of the results; repeats gave similar results.

(16). According to the EUCAST database, the theoretical AZM epidemiological cut-off value for *E. coli* is 16 μg/mL (34). Our wild-type *E. coli* MG1655 strain has an AZM plate MIC of 16 μg/mL, and R717Q/L mutants 64 and 128 μg/mL, respectively (Table 1). Mutants also have an AZM liquid MIC of 128 μg/mL (Fig. 2). These substitutions caused a hydrophilicity decrease at the entrance of the PBP (Fig. 1, 5, S5). Gln is polar while Leu is hydrophobic; still, both substitutions cause macrolide MIC increases. Macrolides are hydrophobic molecules; thus, the hydrophilicity decrease (and the removal of a positive charge) partly explains the increased resistance. Additionally, the side chains are significantly shorter for R717Q/L, enlarging the PBP entrance (Fig. 1c, Fig. 5), further explaining the enhanced efflux of bulky macrolides (13). We showed that bulky Trp substitutions at the PBP entrance decreased ERY MICs significantly (14), corroborating

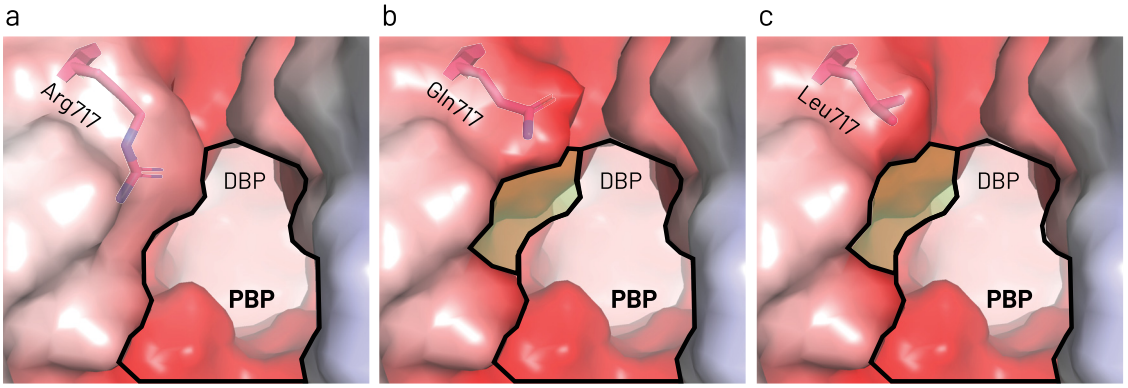

FIG 5 Comparison of the entrance area of the proximal binding pocket in the Access (or Loose [L]) monomer of AcrB-Ec for wild-type and the mutants. (a) Wild-type, (b) R717Q mutant, and (c) R717L mutant AcrB-Ec. (a–c) The residues of interest are depicted as pink sticks. The electrostatic surface is depicted from red to blue. The bold lines indicate the wild-type AcrB-Ec proximal binding pocket entrance area at the Arg717 location. In (b) and (c), the green highlighted area depicts the increased area for R717Q (Gln717) and R717L (Leu717) mutant AcrB-Ec, respectively. These images show the entrance of the proximal binding pocket, leading to the distal binding pocket in the background. PBP, proximal binding pocket; DBP, distal binding pocket. PDB accession code: 4DX5.

the impact of space-limiting substitutions on macrolide-export. The increased space and the increased hydrophobicity can explain why R717L seems slightly more active in exporting macrolides than R717Q (Table 1, Fig. 2). Furthermore, the inhibition zone for R717L was also significantly smaller than for R717Q for fluoroquinolones and MIN (Fig. 4). Basically no difference was found between the mutants on the growth under CLX, while R717L seemed slightly more viable than R717Q under NOV (Fig. 3).

As explained, besides increased macrolide and fluoroquinolone resistance, we observed decreased MICs for CLX and NOV. Therefore, it may be clinically interesting to combine multiple antibiotics to treat typhoid and paratyphoid fever to mitigate resistance and enhance treatment. For example, a combination of β-lactams and AZM may enhance the treatment of *Salmonella* infections. Additionally, we observed this significant gain-of-function in *E. coli* AcrB for the first time, showing that these mutations in other pathogenic bacteria may significantly affect clinical treatment options. These results further imply the importance of adjusted antibiotics treatments, and the need for novel antibiotics and efflux pump inhibitors.

E. coli MG1655 (35) was used to create Δ*acrB* (NKE96) (36) by gene deletion (37). Bacterial strains were grown at 37°C in Luria-Bertani broth (38). His-tagged AcrB was expressed from pBAD33acrBhis, and point mutations were introduced by PCR (GenScript). Susceptibility testing in liquid and on solid media was determined by adding the toxic compounds by serial dilutions. Cell cultures (supplemented with 10 mM arabinose) were incubated until $OD_{600\ nm}$ 0.6 and diluted to 0.05. For liquid growth curves, $OD_{600\ nm}$ readings were performed. For LB agar experiments, cells were stamped on agar plates and incubated overnight. Disk diffusion susceptibility was performed according to (39, 40), with slight modifications. In short: Mueller-Hinton agar plates were supplemented with resazurin (41). Overnight cultures were diluted and grown until $OD_{600\ nm}$ 0.6, and then diluted to $OD_{600\ nm}$ 0.1 with PBS buffer. Cells were streaked, and antibiotic discs were added. Plates were left overnight at 37°C (42).

Data availability. Data are available in the published article itself, and the supporting figures and tables are available as supplemental material. Other data that support the findings of this study are available from the corresponding authors upon request.

SUPPLEMENTAL MATERIAL

Supplemental material is available online only.

SUPPLEMENTAL FILE 1, PDF file, 4.4 MB.

ACKNOWLEDGMENTS

This research was supported by the Center of Innovation Program (COI) from the Japan Science and Technology Agency (JST), Grant-in-Aid for Scientific Research (Early-Career Scientists) (Kakenhi 20K16242), Grant-in-Aid for Scientific Research (Challenging Research (Exploratory)) (Kakenhi 18K19451) from the Japan Society for the Promotion of Science (JSPS), CREST (JPMJCR20H9), the Takeda Science Foundation, the International Joint Research Promotion Program of Osaka University, and the Dynamic Alliance for Open Innovation Bridging Human, Environment and Materials from the Ministry of Education, Culture, Sports, Science and Technology—Japan (MEXT).

REFERENCES

1. World Health Organization. 2015. Global action plan on antimicrobial resistance. World Health Organization: Geneva, Switzerland. https://www.who.int/publications/i/item/9789241509763. Accessed 01 December 2021.
2. Blair JMA, Webber MA, Baylay AJ, Ogbolu DO, Piddock LJV. 2015. Molecular mechanisms of antibiotic resistance. Nat Rev Microbiol 13:42–51. https://doi.org/10.1038/nrmicro3380.
3. World Health Organization. 2014. Antimicrobial resistance global report on surveillance: 2014 summary. World Health Organization: Geneva, Switzerland. https://apps.who.int/iris/handle/10665/112642. Accessed 01 December 2021.
4. Walsh C. 2003. Where will new antibiotics come from? Nat Rev Microbiol 1:65–70. https://doi.org/10.1038/nrmicro727.
5. Allen HK, Donato J, Wang HH, Cloud-Hansen KA, Davies J, Handelsman J. 2010. Call of the wild: antibiotic resistance genes in natural environments. Nat Rev Microbiol 8:251–259. https://doi.org/10.1038/nrmicro2312.
6. Levy SB, Marshall B. 2004. Antibacterial resistance worldwide: causes, challenges and responses. Nat Med 10:S122–S129. https://doi.org/10.1038/nm1145.
7. Blair JMA, Richmond GE, Piddock LJV. 2014. Multidrug efflux pumps in Gram-negative bacteria and their role in antibiotic resistance. Future Microbiol 9:1165–1177. https://doi.org/10.2217/fmb.14.66.
8. Nikaido H. 2009. Multidrug resistance in bacteria. Annu Rev Biochem 78:119–146. https://doi.org/10.1146/annurev.biochem.78.082907.145923.

9. Li X-Z, Plésiat P, Nikaido H. 2015. The challenge of efflux-mediated antibiotic resistance in gram-negative bacteria. Clin Microbiol Rev 28:337–418. https://doi.org/10.1128/CMR.00117-14.
10. Nikaido H. 1996. Multidrug efflux pumps of Gram-negative bacteria. J Bacteriol 178:5853–5859. https://doi.org/10.1128/jb.178.20.5853-5859.1996.
11. Zwama M, Yamaguchi A. 2018. Molecular mechanisms of AcrB-mediated multidrug export. Res Microbiol 169:372–383. https://doi.org/10.1016/j.resmic.2018.05.005.
12. Zwama M, Nishino K. 2021. Ever-adapting RND efflux pumps in Gram-negative multidrug-resistant pathogens: a race against time. Antibiotics 10:774. https://doi.org/10.3390/antibiotics10070774.
13. Nakashima R, Sakurai K, Yamasaki S, Nishino K, Yamaguchi A. 2011. Structures of the multidrug exporter AcrB reveal a proximal multisite drug-binding pocket. Nature 480:565–569. https://doi.org/10.1038/nature10641.
14. Zwama M, Yamasaki S, Nakashima R, Sakurai K, Nishino K, Yamaguchi A. 2018. Multiple entry pathways within the efflux transporter AcrB contribute to multidrug recognition. Nat Commun 9:124. https://doi.org/10.1038/s41467-017-02493-1.
15. Duy PT, Dongol S, Giri A, To NTN, Thanh HND, Quynh NPN, Trung PD, Thwaites GE, Basnyat B, Baker S, Rabaa MA, Karkey A. 2020. The emergence of azithromycin-resistant *Salmonella* Typhi in Nepal. JAC Antimicrob Resist 2:dlaa109. https://doi.org/10.1093/jacamr/dlaa109.
16. Iqbal J, Dehraj IF, Carey ME, Dyson ZA, Garrett D, Seidman JC, Kabir F, Saha S, Baker S, Qamar FN. 2020. A race against time: reduced azithromycin susceptibility in *Salmonella enterica* serovar Typhi in Pakistan. mSphere 5:e00215-20. https://doi.org/10.1128/mSphere.00215-20.
17. Molloy A, Nair S, Cooke FJ, Wain J, Farrington M, Lehner PJ, Torok ME. 2010. First Report of *Salmonella enterica* serotype Paratyphi A azithromycin resistance leading to treatment failure. J Clin Microbiol 48:4655–4657. https://doi.org/10.1128/JCM.00648-10.
18. Parry CM, Thieu NTV, Dolecek C, Karkey A, Gupta R, Turner P, Dance D, Maude RR, Ha V, Tran CN, Thi PL, Be BPV, Phi LTT, Ngoc RN, Ghose A, Dongol S, Campbell JI, Thanh DP, Thanh TH, Moore CE, Sona S, Gaind R, Deb M, Anh HV, Van SN, Tinh HT, Day NPJ, Dondorp A, Thwaites G, Faiz MA, Phetsouvanh R, Newton P, Basnyat B, Farrar JJ, Baker S. 2015. Clinically and microbiologically derived azithromycin susceptibility breakpoints for *Salmonella enterica* serovars Typhi and Paratyphi A. Antimicrob Agents Chemother 59:2756–2764. https://doi.org/10.1128/AAC.04729-14.
19. Hooda Y, Sajib MSI, Rahman H, Luby SP, Bondy-Denomy J, Santosham M, Andrews JR, Saha SK, Saha S. 2019. Molecular mechanism of azithromycin resistance among typhoidal *Salmonella* stains in Bangladesh identified through passive pediatric surveillance. PLoS Negl Trop Dis 13:e0007868. https://doi.org/10.1371/journal.pntd.0007868.
20. Katiyar A, Sharma P, Dahiya S, Singh H, Kapil A, Kaur P. 2020. Genomic profiling of antimicrobial resistance genes in clinical isolates of *Salmonella* Typhi from patients infected with Typhoid fever in India. Sci Rep 10:8299. https://doi.org/10.1038/s41598-020-64934-0.
21. Sajib MSI, Tanmoy AM, Hooda Y, Rahman H, Andrews JR, Garrett DO, Endtz HP, Saha SK, Saha S. 2021. Tracking the emergence of azithromycin resistance in multiple genotypes of typhoidal *Salmonella*. mBio 12:e03481-20. https://doi.org/10.1128/mBio.03481-20.
22. Lyu M, Moseng MA, Reimche JL, Holley CL, Dhulipala V, Su C-C, Shafer WM, Yu EW. 2020. Cryo-EM structures of a gonococcal multidrug efflux pump illuminate a mechanism of drug recognition and resistance. mBio 11:e00996-20. https://doi.org/10.1128/mBio.00996-20.
23. Ma KC, Mortimer TD, Grad YH. 2020. Efflux pump antibiotic binding site mutations are associated with azithromycin nonsusceptibility in clinical *Neisseria gonorrhoeae* isolates. mBio 11:e01509-20. https://doi.org/10.1128/mBio.01509-20.
24. Rouquette-Loughlin CE, Reimche JL, Balthazar JT, Dhulipala V, Gernert KM, Kersh EN, Pham CD, Pettus K, Abrams AJ, Trees DL, Cyr SS, Shafer WM. 2018. Mechanistic basis for decreased antimicrobial susceptibility in a clinical isolate of *Neisseria gonorrhoeae* possessing a mosaic-like *mtr* efflux pump locus. mBio 9:e02281-18. https://doi.org/10.1128/mBio.02281-18.
25. Wadsworth CB, Arnold BJ, Sater MRA, Grad YH. 2018. Azithromycin resistance through interspecific acquisition of an epistasis-dependent efflux pump component and transcriptional regulator in *Neisseria gonorrhoeae*. mBio 9:e01419-18. https://doi.org/10.1128/mBio.01419-18.
26. Blair JMA, Bavro VN, Ricci V, Modi N, Cacciotto P, Kleinekathöfer U, Ruggerone P, Vargiu AV, Baylay AJ, Smith HE, Brandon Y, Galloway D, Piddock LJV. 2015. AcrB drug-binding pocket substitution confers clinically relevant resistance and altered substrate specificity. Proc Natl Acad Sci U S A 112:3511–3516. https://doi.org/10.1073/pnas.1419939112.
27. Zwama M, Yamaguchi A, Nishino K. 2019. Phylogenetic and functional characterisation of the *Haemophilus influenzae* multidrug efflux pump AcrB. Commun Biol 2:340. https://doi.org/10.1038/s42003-019-0564-6.
28. Murakami S, Nakashima R, Yamashita E, Matsumoto T, Yamaguchi A. 2006. Crystal structures of a multidrug transporter reveal a functionally rotating mechanism. Nature 443:173–179. https://doi.org/10.1038/nature05076.
29. Nakashima R, Sakurai K, Yamasaki S, Hayashi K, Nagata C, Hoshino K, Onodera Y, Nishino K, Yamaguchi A. 2013. Structural basis for the inhibition of bacterial multidrug exporters. Nature 500:102–106. https://doi.org/10.1038/nature12300.
30. Morgan CE, Glaza P, Leus IV, Trinh A, Su C-C, Cui M, Zgurskaya HI, Yu EW. 2021. Cryoelectron microscopy structures of AdeB illuminate mechanisms of simultaneous binding and exporting of substrates. mBio 12:e03690-20. https://doi.org/10.1128/mBio.03690-20.
31. Eicher T, Cha H, Seeger MA, Brandstätter L, El-Delik J, Bohnert JA, Kern WV, Verrey F, Grütter MG, Diederichs K, Pos KM. 2012. Transport of drugs by the multidrug transporter AcrB involves an access and a deep binding pocket that are separated by a switch-loop. Proc Natl Acad Sci U S A 109:5687–5692. https://doi.org/10.1073/pnas.1114944109.
32. Tam H-K, Foong WE, Oswald C, Herrmann A, Zeng H, Pos KM. 2021. Allosteric drug transport mechanism of multidrug transporter AcrB. Nat Commun 12:3889. https://doi.org/10.1038/s41467-021-24151-3.
33. Ornik-Cha A, Wilhelm J, Kobylka J, Sjuts H, Vargiu AV, Malloci G, Reitz J, Seybert A, Frangakis AS, Pos KM. 2021. Structural and functional analysis of the promiscuous AcrB and AdeB efflux pumps suggests different drug binding mechanisms. Nat Commun 12:6919. https://doi.org/10.1038/s41467-021-27146-2.
34. EUCAST. Antimicrobial wild type distributions of microorganisms. https://mic.eucast.org. Accessed 01 December 2021.
35. Blattner FR, Plunkett G, Bloch CA, Perna NT, Burland V, Riley M, Collado-Vides J, Glasner JD, Rode CK, Mayhew GF, Gregor J, Davis NW, Kirkpatrick HA, Goeden MA, Rose DJ, Mau B, Shao Y. 1997. The complete genome sequence of *Escherichia coli* K-12. Science 277:1453–1462. https://doi.org/10.1126/science.277.5331.1453.
36. Senda Y, Yamaguchi A, Nishino K. 2008. The AraC-family regulator GadX enhances multidrug resistance in *Escherichia coli* by activating expression of *mdtEF* multidrug efflux genes. J Infect Chemother 14:23–29. https://doi.org/10.1007/s10156-007-0575-y.
37. Datsenko KA, Wanner BL. 2000. One-step inactivation of chromosomal genes in *Escherichia coli* K-12 using PCR products. Proc Natl Acad Sci U S A 97:6640–6645. https://doi.org/10.1073/pnas.120163297.
38. Sambrook J, Fritsch EF, Maniatis T. 1989. Molecular cloning: a laboratory manual, 2nd ed. Cold Spring Harbor Laboratory Press, Cold Spring Harbor, NY.
39. Bauer AW, Kirby WMM, Sherris JC, Turck M. 1966. Antibiotic susceptibility testing by a standardized single disk method. Am J Clin Pathol 45:493–496. https://doi.org/10.1093/ajcp/45.4_ts.493.
40. Kirby WM, Yoshihara GM, Sundsted KS, Warren JH. 1956. Clinical usefulness of a single disc method for antibiotic sensitivity testing. Antibiotics Annu 1956–1957:892–897.
41. Sener S, Acuner IC, Bek Y, Durupinar B. 2011. Colorimetric-plate method for rapid disk diffusion susceptibility testing of *Escherichia coli*. J Clin Microbiol 49:1124–1127. https://doi.org/10.1128/JCM.02104-10.
42. Hudzicki J. 2009. Kirby-Bauer disk diffusion susceptibility test protocol. American Society for Microbiology, Washington, DC.